Multinuclear NMR studies of mixed $Ca_{1-x}Sr_xF_2$ crystals

R. E. Youngman* and C. M. Smith
Science & Technology, Corning Incorporated, Corning, New York 14831, USA
(Received 27 May 2008; published 24 July 2008)

The local environments of fluorine and calcium ions in $Ca_{1-x}Sr_xF_2$ single crystals have been studied using ^{19}F and ^{43}Ca magic-angle spinning (MAS) NMR spectroscopies. The fluorine speciation is found to depend on both the distribution of cations (Ca and Sr) around each fluorine site in the fluorite lattice, as well as fluctuations in the ionic character of bonding between fluorine and these cations. The natural abundance ^{43}Ca MAS NMR results show a clear relation between ^{43}Ca chemical shielding and bond distances in halides, with increasing shielding as the fluorite lattice expands and Ca-F distances lengthen. When taken together, the results from ^{19}F and ^{43}Ca NMR are consistent with a random substitution of Sr for Ca in the mixed fluoride system.

DOI: 10.1103/PhysRevB.78.014112 PACS number(s): 61.05.Qr, 61.66.Fn

I. INTRODUCTION

The alkaline-earth fluoride crystals (Ca, Sr, and Ba)F_2 have wide optical band gaps that make them appropriate for optical applications from the vacuum UV(<200 nm) (VUV) through the infrared (>10 μm) regions.[1] Their VUV transparency is found to decrease with increasing atomic number;[2] accordingly, refractive index is found to increase with increasing atomic number.[3] Because of their high transparency in the VUV, these materials have been considered for use in short-wavelength lithography using 193 or 157 nm light.[4,5] It was found, however, that these crystals exhibit a property referred to as "intrinsic birefringence"[6] or "spatial dispersion" at short wavelength. In classical crystal optics, cubic materials, such as these alkaline-earth fluorides, are considered to be optically isotropic—with their refractive indices independent of direction. This is a simplification, however, that breaks down in certain regimes. Specifically, when the interrogation wavelength is sufficiently short and/or the refractive index at the wavelength is sufficiently high, cubic crystals do exhibit birefringence.[7,8] This is a consequence of polarization being influenced not only by the local field at a given point but also by the closest neighborhood around that point. Birefringence is then dependent not only on frequency but also on the wave vector.

Intrinsic birefringence of CaF_2, SrF_2, and BaF_2 has been measured from 365 to 156 nm (Refs. 6 and 9). Values at 156 and 193 nm are shown in Table I, which are reproduced from Ref. 9. Inspection of these data reveals that the sign of the birefringence is negative for CaF_2 at both wavelengths and positive at both wavelengths for the two fluorides containing cations of higher ionic polarizability (Sr and Ba). Birefringence of any origin (stress or intrinsic) can be a limiting property for short-wavelength imaging applications. While stress birefringence can be minimized by annealing procedures, intrinsic birefringence would need to be managed by other methods. Potential solutions include clocking lens elements relative to each other; that is, rotating a second element of the same composition and crystal orientation appropriately so that the birefringence of the whole is minimized.[6] Alternatively, given the different signs of birefringence for the different fluorides, one could incorporate different crystals having intrinsic birefringence of opposite sign into one lens assembly; the effect would be to have the positive birefringence of one "cancel out" the negative birefringence of the other.[10] A scheme that involves using stress-induced photoelastic birefringence to compensate for the intrinsic birefringence has also been described.[11] Finally, one could actually obtain an optically isotropic material of a cubic crystal by preparing mixed crystals, containing the appropriate amounts of alkaline-earth ions (calcium plus appropriate amounts of Sr and/or Ba) (Refs. 9, 12, and 13). If the mixing of the cations is sufficiently random, the symmetry that gives rise to the intrinsic birefringence in the pure compounds would be broken and the final material would have lowered intrinsic birefringence. Using the data in Table I, a mixed crystal of the composition $Ca_{0.66}Sr_{0.34}F_2$ would have no intrinsic birefringence at 193 nm (Ref. 9).

In our exploration of mixed crystals containing Sr and Ca cations, we have previously reported on Raman and ^{19}F NMR studies.[14] In that paper, we observed a single Raman band for all compositions studied, consistent with a random mixing of the cations, and in accordance with the findings reported in Ref. 15. The ^{19}F NMR results supported that conclusion and additionally showed the existence of different fluorine environments in the mixed crystals, which is attributed to changes in the cation distribution around fluorine. In the present work, we expand on the ^{19}F NMR findings and include an examination of the atomic structure from the cation perspective using natural abundance ^{43}Ca magic-angle spinning (MAS) NMR. These data confirm the random substitution of Sr for Ca in the fluorite crystal lattice, and the observation of a single resonance for each composition is consistent with homogeneity over the sampled volume.

TABLE I. Magnitude and sign of the intrinsic birefringence of pure alkaline-earth fluoride crystals measured at 193 and 156 nm (Ref. 9).

Material	$\Delta n \times 10^7$ (193 nm)	$\Delta n \times 10^7$ (156 nm)
CaF_2	-3.4 ± 0.2	-11.8 ± 0.4
SrF_2	$+6.6 \pm 0.2$	$+5.7 \pm 0.3$
BaF_2	$+19 \pm 2$	$+33 \pm 3$

TABLE II. Compositions and lattice constants for the five mixed fluoride crystals examined in this work.

Sample	CaF_2 (mol %)	SrF_2 (mol %)	Lattice Constant (Å)
A	74	26	5.55
B	44	56	5.66
C	24	76	5.72
D	13	87	5.76
E	5	95	5.78

Moreover, while natural abundance ^{43}Ca NMR has been reported on a variety of crystalline compounds,[16–20] these results demonstrate the effect of calcium-halide bond distances on the ^{43}Ca chemical shielding and thus will add to our understanding of this critically important (but seldom studied) nuclide by conventional and natural abundance NMR methodology.

II. EXPERIMENT

A. Sample preparation and basic characterization

The single mixed crystals were grown using the vacuum Stockbarger technique. The Ca and Sr fluoride starting materials were premixed with a metal-fluoride oxygen getter. The mixture was premelted to yield densified bulk material, which was essentially free of oxygen contamination. This material was then charged into crucibles for the crystal-growth step. The crystals were grown using an oriented seed crystal while lowering the crucible through a temperature gradient. The cation compositions of the mixed crystals were determined by traditional wet chemical methods and were reported in Table II. X-ray powder diffraction was used to obtain lattice constants and was also given in Table II.

B. Nuclear magnetic resonance

The ^{19}F NMR spectra were collected using a commercial spectrometer in conjunction with an 11.7 T superconducting magnet. The resonance frequency of ^{19}F at this field was 470.3 MHz. Samples were ground into powders and packed into 2.5 mm zirconia rotors for MAS NMR, with spinning speeds of nominally 27 kHz. The spectra were acquired using a $\pi/2$ pulse width of 0.8 μs, recycle delay of 30 s, and signal averaging of 1000 acquisitions. The data were processed without additional line broadening and plotted against the chemical shift of $CFCl_3$ at 0 ppm. Quantitative analysis of the ^{19}F MAS NMR spectra was performed using commercial software and involved fitting of all isotropic resonances and their associated spinning sidebands.

The ^{43}Ca MAS NMR spectra were collected on fluoride crystals without the aid of isotopic enrichment. These experiments were performed at 11.7 T (33.6 MHz resonance frequency) using a 9.5 mm MAS NMR probe. Samples were powdered and packed into 9.5 mm zirconia rotors, with sample spinning rates of 3–4 kHz. Data were acquired using 5.0 μs pulse widths (approximately $\pi/4$) and recycle delays of 2 s. The signal averaging for these experiments was varied with CaF_2 content of the samples and ranged between 94 000 and 320 000 scans. The spectra were processed with line broadening commensurate with the signal/noise quality and was either 33 or 100 Hz, the latter used only for the lowest CaF_2-containing sample. Due to minor probe ringing at this resonance frequency, several of the initial free-induction-decay points were backward linear predicted using CHEMAGNETICS SPINSIGHT software to achieve a relatively flat baseline. By varying the number of such points, we established that this processing protocol does not alter the frequency or width of the detected NMR signals, both of which are necessary for estimating ^{43}Ca isotropic chemical shift (δ_{iso}) values. The ^{43}Ca NMR spectra were plotted against an external shift reference (saturated aqueous solution of $CaCl_2$) at 0 ppm.

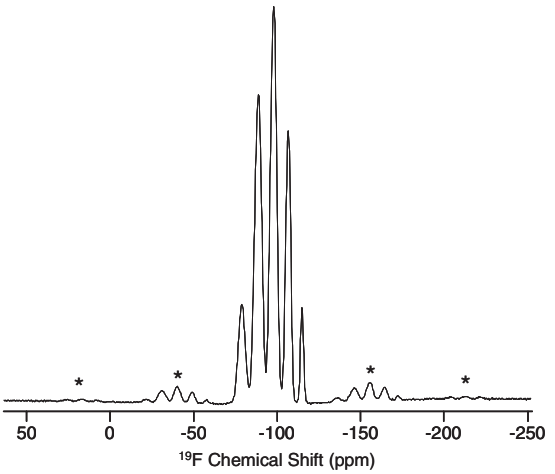

FIG. 1. ^{19}F MAS NMR spectrum of the $Ca_{0.44}Sr_{0.56}F_2$ crystal with the entire spinning sideband manifold. The asterisks denote spinning sidebands.

III. RESULTS

Compositions from wet chemistry measurements and lattice constants from powder x-ray diffraction (XRD) are shown in Table II. The lattice constants from XRD vary smoothly as the amount of SrF_2 is increased, reaching a value of 5.78 Å for the crystal having the highest SrF_2 content (sample E).

The ^{19}F MAS NMR spectrum of the $Ca_{0.44}Sr_{0.56}F_2$ crystal (sample B) is plotted in Fig. 1. This spectrum consists of a cluster of isotropic peaks between −70 and −115 ppm, with spinning sidebands displaced by the spinning frequency (27 kHz or ~57 ppm).

The ^{19}F MAS NMR spectra for the entire series of mixed crystals, as well as both end-member compositions, are given in the stack plot of Fig. 2. Pure CaF_2 contains a single resonance at −108.6 ppm, consistent with previously reported data.[21,22] As SrF_2 is added, additional fluorine resonances are detected, and both their frequency and relative intensities vary with composition. The entire manifold of isotropic peaks shifts to lower chemical shielding with increasing SrF_2 and approaches the value for pure SrF_2 (−88.1 ppm).

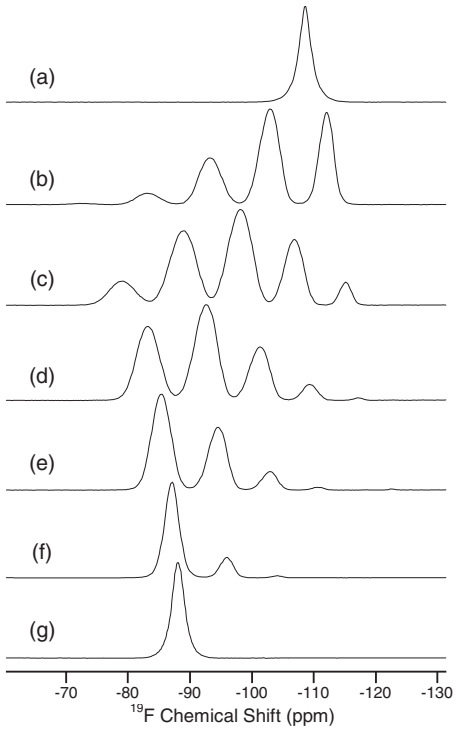

FIG. 2. Expanded ^{19}F MAS NMR spectra of the mixed fluoride crystals showing the isotropic peaks for (a) pure CaF_2, (b) $Ca_{0.74}Sr_{0.26}F_2$, (c) $Ca_{0.44}Sr_{0.56}F_2$, (d) $Ca_{0.24}Sr_{0.76}F_2$, (e) $Ca_{0.13}Sr_{0.87}F_2$, (f) $Ca_{0.05}Sr_{0.95}F_2$, and (g) pure SrF_2.

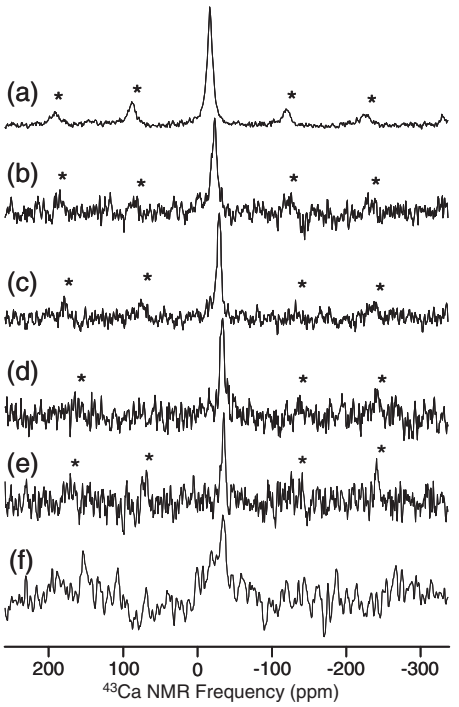

FIG. 3. ^{43}Ca MAS NMR spectra of the mixed fluoride crystals; (a) pure CaF_2, (b) $Ca_{0.74}Sr_{0.26}F_2$, (c) $Ca_{0.44}Sr_{0.56}F_2$, (d) $Ca_{0.24}Sr_{0.76}F_2$, (e) $Ca_{0.13}Sr_{0.87}F_2$, and (f) $Ca_{0.05}Sr_{0.95}F_2$. Spinning sidebands are denoted with asterisks.

The ^{43}Ca MAS NMR spectra are plotted in Fig. 3 for the mixed crystals and pure CaF_2. The spectrum for the latter is consistent with published data having a single ^{43}Ca resonance at −17.6 ppm (Ref. 17). The spectra for the mixed crystals are characterized by a single ^{43}Ca NMR peak, which shifts towards higher shielding as the SrF_2 content is raised. Although signal-to-noise levels for some of the natural abundance ^{43}Ca NMR spectra are less than optimal, all indications show that these data are comprised of only a single narrow resonance.

IV. DISCUSSION

Calcium and strontium fluoride are known to form solid solutions with unlimited mutual solubility.[23,24] The structure of the alkaline-earth fluorides, including mixed Ca and Sr crystals, is that of fluorite. The unit cell is described as a face-centered-cubic lattice of cations (Ca and/or Sr), each coordinated by eight fluorine atoms. The coordination number of fluorine is four. The bond distances and lattice parameters are well characterized for the end-member compositions of this study, CaF_2 and SrF_2. Since the symmetry is cubic, the size of the unit cell is defined by a single lattice parameter a, which describes the length on each edge of the cube. This parameter increases from 5.463 to 5.78 Å for pure CaF_2 and SrF_2, respectively.

According to Vegard's law,[25] the lattice parameters and composition are linearly related for solid solutions like the mixed Ca and Sr fluoride system. This would therefore allow one to predict the lattice constants for the mixed crystals based on a linear interpolation between the values for CaF_2 and SrF_2. Rather than predicting these values, lattice parameters were experimentally determined for the five compositions of this study and are given in Table I. A plot of lattice parameter versus composition is shown in Fig. 4, where a perfectly linear relationship does indeed hold for these materials, consistent with other published findings.[15,26] This

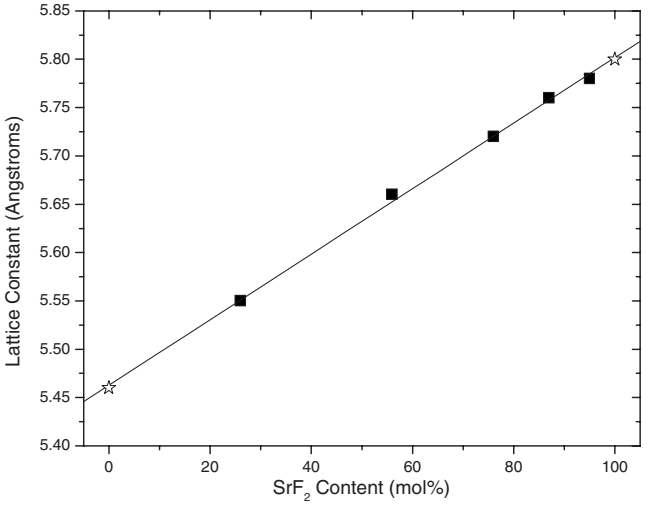

FIG. 4. Plot of lattice constant from XRD versus composition of the mixed fluoride crystals. The solid curve represents a linear fit to these data. Uncertainties are within the size of the symbols.

confirms that as Sr replaces Ca in the fluorite crystal structure, the overall size of the unit cell expands to accommodate the larger cation.

The lattice-parameter data in Fig. 4 also confirm that we have random substitution of SrF_2 in the CaF_2 lattice. Had the added SrF_2 formed clusters or nonhomogeneous decoration of the crystalline lattice, we would have likely observed deviation from Vegard's Law and certainly detected multiple unit cells in the experimental x-ray diffraction data. In addition, our prior study of this solid solution contained Raman spectroscopic evidence for random substitution of Sr for Ca (Ref. 14). A single vibrational band was measured for all compositions, showing a linear frequency dependence and, therefore, homogeneity in the Ca-Sr distribution. The detection of a single Raman band, as well as XRD data on the mixed crystals, also confirms that cubic symmetry is maintained throughout the entire solid solution, which will be an important point in interpreting the NMR data below. The Raman and x-ray supports for homogeneous random mixtures of CaF_2 and SrF_2 are consistent with the previous studies of this solid solution.[15]

The ^{19}F NMR data on the Ca and Sr mixed crystals were only recently reported and showed surprisingly complex spectra for what seems to be a simple-cubic crystalline lattice.[14] The spectra of pure CaF_2 and SrF_2 are very simple, each containing a single fluorine resonance at −108 and −88.1 ppm, respectively. These shifts are generally consistent with those reported in the literature, although the range of values for SrF_2 spans several parts per million.[21,27–29] As soon as SrF_2 is introduced into the CaF_2 lattice, the ^{19}F MAS NMR spectra show significant complexity. These data are typically characterized by a cluster of isotropic resonances shown in Fig. 1 for the $Ca_{0.44}Sr_{0.56}F_2$ crystal, where peaks are detected at chemical shifts of −79.0, −88.9, −98.1, −106.8, and −115.1 ppm. The peaks are well resolved and can be fit using Gaussian lineshapes. From these fits, including all spinning sidebands, the relative peak intensities are readily obtained (Table III).

Assignment of these five fluorine resonances is straightforward when one considers the fluorite crystal structure. For each fluorine atom, there are five different ways to distribute a combination of Ca and Sr cations as nearest neighbors: all Ca, all Sr, 3Ca/1Sr, 2Ca/2Sr, and 1Ca/3Sr. Each of these distributions gives rise to a unique ^{19}F chemical shift, since the shielding is roughly linear with ionic radii in the alkaline-earth fluorides.[29] In addition, the spectral intensity distribution amongst the different resonances can be explained by the proposed random distribution of cations surrounding a particular F atom. In the case of sample B with 44 mol % of CaF_2, the random distribution of cations in the fluorite lattice gives a statistical population of 10, 31, 38, 18, and 3 for the five fluorine sites on going from all Sr to all Ca cation neighbors, in good agreement with the experimental values in Table III. The ^{19}F NMR data for the other mixed crystals were similarly analyzed in terms of peak intensity distributions, and in all cases, the high level of agreement between the measured and predicted intensities confirmed the random distribution of Sr and Ca throughout the crystal.

The other interesting result from the fluorine perspective is that the ^{19}F chemical shielding is not only delineated by the ways in which one can surround the fluoride by Ca and Sr, but also that the ^{19}F chemical shift values of each unique site change with composition. As can be seen in Fig. 2, the ^{19}F resonance due to fluorine with 2Ca and 2Sr neighbors, for example, does not remain fixed for all crystal compositions. This particular resonance varies between −93 and −104 ppm for crystals containing 26 and 95 mol % of SrF_2 (Table III). This variation, while not large on the overall scale of ^{19}F chemical shielding, does suggest a more complex influence on chemical shielding than simply the nearest-neighbor cation distribution. Further evidence of this suggestion is shown in Fig. 5, where the ^{19}F chemical shifts of the five distinct fluorine peaks are plotted as a function of the mole fraction of CaF_2. Each resonance appears to have a linear dependence on the crystal composition and thus a linear change with lattice size. Therefore, the shift of each distinct fluorine environment, defined by its cation neighbor distribution, is dependent on the separation between fluorine and these cations. The trend for a fluorine surrounded by all Ca neighbors (filled squares in Fig. 5) is extrapolated to include the chemical shift of ^{19}F in pure CaF_2. In this case, the ^{19}F chemical shift appears at −107.5 ppm for CaF_2 and be-

TABLE III. ^{19}F and ^{43}Ca NMR parameters for the mixed fluoride crystals using the sample designations of Table II. The ^{19}F peak intensities include all spinning sidebands. The ^{43}Ca chemical shifts were estimated from the measured shift values using the method described in Ref. 17.

Sample	^{19}F δ (ppm) (±0.2)	Intensity (%) (±0.2)	^{43}Ca δ_{iso} (ppm)
A	−72.5	0.5	−23.7 ± 0.4
	−83.2	5.8	
	−93.2	23.0	
	−102.9	41.4	
	−112.1	29.2	
B	−79.0	9.9	−29.6 ± 0.5
	−88.9	30.4	
	−98.1	35.8	
	−106.8	19.6	
	−115.1	4.3	
C	−83.2	32.9	−33.4 ± 0.6
	−92.6	41.7	
	−101.2	20.3	
	−109.4	4.6	
	−117.2	0.4	
D	−85.3	55.9	−35.9 ± 0.8
	−94.5	34.8	
	−102.6	8.3	
	−110.7	0.9	
E	−87.1	84.1	−35.2 ± 1
	−95.9	14.8	
	−104.1	1.1	

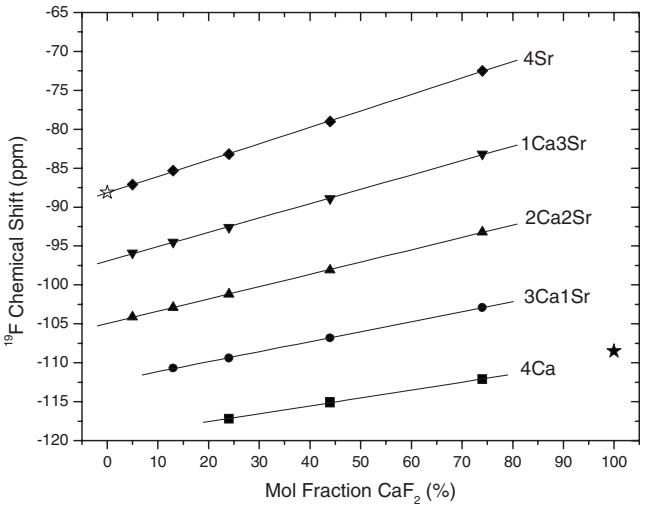

FIG. 5. Plot of ^{19}F chemical shifts in the various mixed fluoride crystals. Assignment of the five ^{19}F resonances follows that in the text and is denoted by the number of Ca and Sr neighbors. The solid curves are linear fits to the data from the mixed Ca and Sr fluoride crystals and do not include the end-member compositions. Uncertainties are within the size of the symbols. The open and closed stars are measured chemical shifts for pure SrF_2 and CaF_2, respectively.

comes more shielded upon addition of SrF_2 and concomitant expansion of the cubic lattice. The other fluorine resonances in the mixed Ca and Sr fluoride crystals show a similar increase in shielding with increasing lattice size. Assuming that the lattice expansion correlates with an increase in fluorine-cation bond distance, the trends in ^{19}F chemical shift indicate a shielding of the resonance with increasing distance, contrary to what is usually observed in bond distance versus chemical shielding correlations in metal fluorides.[29]

The lack of a fixed shift for each peak is consistent with a random arrangement of cations at length scales beyond nearest neighbor. Since the identity of nearest-neighbor cations has a pronounced effect on fluorine shielding, it can be argued that cations in next-nearest-neighbor positions might also influence the chemical shift. If those cations were always of the same identity that would necessarily imply an ordered system and would yield the same chemical shift for all compositions. For example, if a fluorine atom with 2Ca and 2Sr neighbors always had the same distribution of cations within the next sphere, then the material would be more ordered and the fluorine chemical shift would remain constant. This is in opposition to what we observe.

To this end, it is apparent that changes in chemical shielding of the five distinct fluorine resonances in the Ca and Sr fluoride solid solution are not simply dictated by short-range geometrical changes (i.e., varying bond distances), but likely involve more subtle electronic effects. The contribution of second-neighbor fluorine atoms has been incorporated into theoretical studies of fluorine chemical shielding in alkaline-earth fluorides, and was shown to be an important factor in gaining agreement between *ab initio* and experimental results.[30] In this study, the size dependence of cluster models was shown to impact the calculated shielding of fluorine by as much as 50 ppm, suggesting that the neighboring fluorines do influence the chemical shift of a given fluorine atom. In view of this observation, one could envisage a situation in which a fluorine with four Ca neighbors is surrounded by other fluorines with slightly different cation neighbors, such as a mixture of Ca and Sr. The local shielding of the mixed coordination fluorine is lower than the pure CaF_2 environment, which could then impact how the "shared" Ca cation is bonded with the fluorine of interest. Theoretical treatments of the Ca and Sr fluoride solid solutions are beyond the scope of this experimental study, but it may provide a better understanding of the changes in fluorine chemical shielding in fluoride solid solutions.

Another possible explanation for the trends in Fig. 5, consistent with proposed effects due to second neighbors, comes from two studies of fluoride-containing systems. In the first set,[27,31] covalency and electronic configuration arguments were used to understand chemical shielding of fluorine in difluoride compounds. In highly ionic systems such as the alkaline-earth fluorides, the extent of covalent interaction between cation and fluorine has a pronounced influence on the fluorine chemical shift. Vaughan *et al.*[27] plotted ^{19}F chemical shielding for the alkaline-earth fluorides versus a covalency parameter and cation electronegativities, obtaining linear trends for both. Their findings indicated a large change in fluorine chemical shielding with small changes in covalency or essentially the degree of ionic bonding between fluorine and the alkaline-earth cation. This treatment of the large chemical shift range in group II cubic difluorides may also account for the small changes in chemical shift for each given fluorine resonance in the mixed Ca and Sr fluoride crystals. Sites having a majority of Ca neighbors (4 and 3)Ca experience a gradual increase in chemical shielding with increasing SrF_2 content, which corresponds to a slight decrease in bonding covalency. Conversely, those fluorine sites with mostly Sr neighbors experience a deshielding when the lattice is diluted with CaF_2, possibly in response to an increase in the covalent character of the Sr-F bonding. It appears from this argument that Ca-F bonding becomes more ionic as Sr-F bonding increases in covalency, thus demonstrating the dependence of fluorine chemical shifts on both the cation type (Ca and Sr) and also the nature of bonding between the fluorine and alkaline-earth cations. In a second ^{19}F NMR study, shielding differences between the heavy and light alkali fluorides in alkali-metal fluorides were described as resulting from cation-anion polarization effects and the degree of covalency.[32]

In order to further understand the changes in atomic-level structure in these mixed crystals, we have obtained natural abundance ^{43}Ca MAS NMR spectra on all Ca-containing samples. The ^{43}Ca MAS NMR spectra are shown in Fig. 3, where a single resonance is detected for all compositions. Each ^{43}Ca resonance is relatively sharp and does not contain any contributions from second-order quadrupolar line broadening, which might be expected for this spin $-7/2$ nuclide. Due to the cubic symmetry of these crystalline materials, such broadening should be quite small. Fortunately, since the isotropic shift of ^{43}Ca in CaF_2 has now been measured at two different field strengths (11.7 T in this study and 14.1 T in Ref. 17), one can estimate the isotropic chemical shift and quadrupolar coupling product (P_Q) using the field depen-

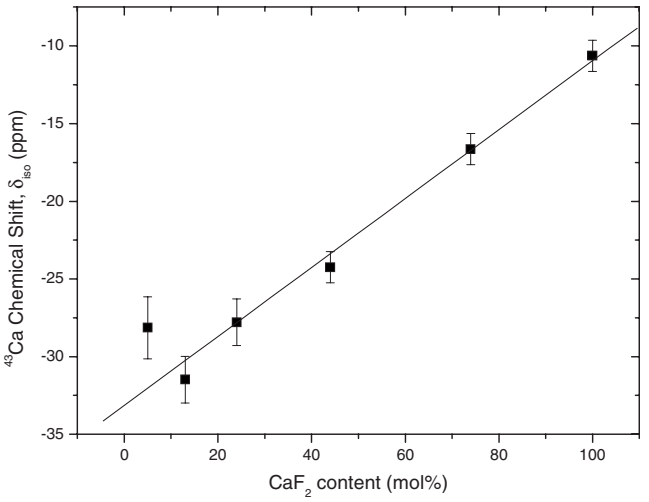

FIG. 6. Plot of ^{43}Ca chemical shift against composition for the mixed fluoride crystals. The solid line is a linear fit to these data and includes all compositions.

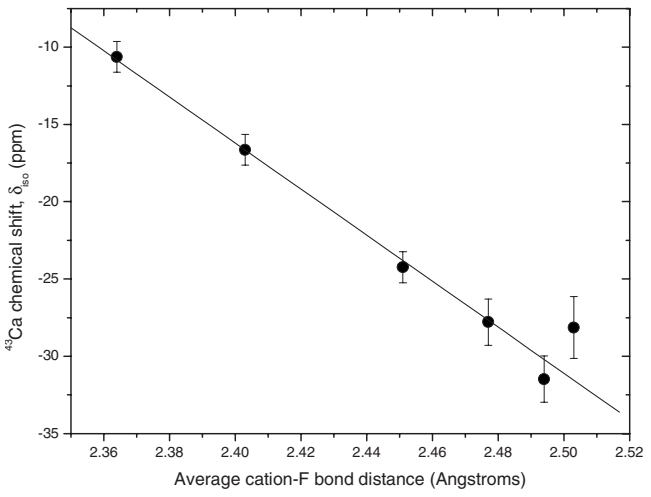

FIG. 7. Plot of ^{43}Ca chemical shift against the average cation-fluorine distance as determined from the lattice parameter of each mixed crystal.

dence of the measured shift.[33,34] Based on these estimates, δ_{CS} and P_Q for ^{43}Ca in pure CaF_2 are −18.9 ppm and 1.39 MHz, respectively, where δ_{CS} is the isotropic chemical shift and P_Q contains both the quadrupolar coupling constant as well as the quadrupolar asymmetry parameter. This chemical shift value differs from the estimate in Ref. 17, where the authors used the residual MAS NMR linewidth to approximate the second-order quadrupolar coupling contribution to the observed frequency of the ^{43}Ca nucleus at a particular external magnetic field. Rather than focusing on a slight discrepancy in chemical shift, which unfortunately may be partial due to the small difference in magnetic-field strength used for these two measurements, it is noted that the quadrupolar coupling constant is small for ^{43}Ca in these cubic crystals. However, the contributions to these resonance frequencies from second-order quadrupolar effects are nonzero and, thus, we have chosen to adopt the methods in Ref. 17 to estimate isotropic chemical shifts for the ^{43}Ca resonances in the mixed crystals (Fig. 3).

As in the case of fluorine shielding, there is a change in ^{43}Ca chemical shift with composition. From the perspective of calcium in the fluorite crystal structure, each cation is surrounded by eight fluorine anions, which does not change upon addition of SrF_2. Some structural models for mixed fluorides assume fixed fluorine-cation distances;[35] however, the bond distances between Ca and fluorine likely depend on the number of Sr cations in the unit cell. Experimentally, it is known that as Sr is substituted for Ca in the fluorite structure, the lattice constant increases (Table II) and, therefore, some changes in fluorine environment (discussed above) and calcium sites would be expected. By plotting the ^{43}Ca shift (Fig. 6), we can see the effect of increasing lattice parameter on the Ca shielding. These data show a linear change in ^{43}Ca shift with composition, with the possibly anomalous result of the mixed crystal having 5% CaF_2. It is possible that the low number of Ca remaining at 5% CaF_2 may already be in an environment surrounded by Sr in several coordination spheres and therefore unaffected by composition. Furthermore, our other data (^{19}F NMR, Raman, and XRD) all strongly support the random mixing of the cations in the mixed crystals and also the homogeneity of the crystals on a macroscopic scale. Given those findings, at this point we attribute any extra ^{43}Ca resonances in the 5% CaF_2 crystals to poor signal quality, and enhancement by the line broadening required to process this particular spectrum. Additional signal averaging or use of isotopic enrichment would aide in evaluation of such features, but both were impractical for this study.

The ^{43}Ca chemical shielding has not been systematically examined in halide systems such as this, where the surrounding anions are fixed and only bond distances and second-nearest neighbors are varied. The only published explanation for shielding changes for ^{43}Ca has been provided by the work of Smith and co-workers,[17] in which they examine the spectra of various oxide and halide systems. These authors, championing the use of natural abundance ^{43}Ca NMR, presented clear evidence for changes in the ^{43}Ca chemical shift of CaF_2, $CaCl_2$, and $CaBr_2$. Unfortunately, they were unable to establish any clear correlation between chemical shift and Ca-halide distance, as changing halide type (i.e., F vs Cl) also introduced differences in electronegativities of the anions, leading to much more complexity than just simple changes in Ca-halide bond distances. The mixed Ca and Sr fluoride crystals in the present study provide a much simpler system in which to understand the effect of Ca-F bond lengths on ^{43}Ca chemical shielding. Given the cubic symmetry of these crystals and making use of the lattice parameters in Table II, one can calculate the average cation-fluorine bond distance,

$$\text{cation-F distance} = \{3(0.25a)^2\}^{1/2},$$

where the lattice parameter a is given in angstroms. This distance between nearest neighbors is similar to that which was used to calculate solid solution hardening in the CaF_2-SrF_2 system.[36] We can therefore plot ^{43}Ca shift as a function of this calculated average bond length in Fig. 7. Assuming that the expanding fluorite lattice leads to a pro-

portional increase in Ca-F bond distance, the data in Fig. 7 therefore show the effect of this changing distance on the ^{43}Ca chemical shielding. The solid curve in Fig. 7 represents a linear fit to the data and gives a slope of −137 ppm/Å. This is consistent with the overall increase in shielding with increasing bond length determined for oxides; however, the absolute change per unit length is roughly half of the value for the oxides.[17] Knowing how bond lengths influence the ^{43}Ca chemical shift in halides will further our ability to make use of this nuclide in studies of inorganic materials.

V. SUMMARY

The ^{19}F and ^{43}Ca NMR studies of mixed Ca and Sr fluoride crystals have shown changes reflecting a random substitution of the cations on the cubic fluorite lattice and adding to the existing spectroscopic and x-ray evidence of this. The experimental evidence is then consistent with the mixed Ca and Sr fluoride system having essentially isotropic properties while in a cubic matrix. The isotropic nature of these materials is a benefit for short-wavelength optical applications.

The complexity in ^{19}F NMR spectra can be accounted for by distributions of Ca and Sr within the four neighboring cation sites and also for a change in bonding configuration between fluorine and these cations. Chemical shielding for ^{43}Ca linearly responds to changes in the unit-cell size and is consistent with the lattice parameter measured by XRD. This study has resulted in a systematic examination of ^{43}Ca shielding in a relatively simple halide system. Since the identity of neighboring anions is fixed throughout the solid solution, changes in ^{43}Ca chemical shielding are due only to changes in Ca-F distances. Shielding at the Ca nucleus is linearly dependent on the distance between Ca and F, and such a trend would presumably hold for other halides. Prior assumptions that cation-fluorine distances do not change in solid solutions of this type must also be reconsidered, particularly when calculating optical or electronic properties.

ACKNOWLEDGMENTS

The authors would like to thank Erika Stapleton and Brett Abel for x-ray diffraction data and for the useful discussion of the lattice parameters in pure CaF_2 and SrF_2; and Bill Rosch for the single crystal of pure SrF_2.

*Author to whom correspondence should be addressed. FAX: 1-607-974-9474; youngmanre@corning.com

[1] R. T. Poole, J. Szajman, R. C. G. Leckey, J. G. Jenkin, and J. Liesegang, Phys. Rev. B **12**, 5872 (1975).
[2] M. Wakaki, K. Kudo, and T. Shibuya, *Physical Properties and Data of Optical Materials* (CRC, New York, 2007).
[3] J. H. Burnett, R. Gupta, and U. Griesmann, Proc. SPIE **4000**, 1503 (2000).
[4] V. Liberman, M. Rothschild, N. N. Efremov, S. T. Palmacci, J. H. C. Sedlacek, C. Van Peski, and K. Orvek, Proc. SPIE **4346**, 45 (2001).
[5] R. W. Sparrow, US Patent No. 6,630,117 (B2) (7 October 2003).
[6] J. H. Burnett, Z. H. Levine, and E. L. Shirley, Phys. Rev. B **64**, 241102(R) (2001).
[7] H. A. Lorentz, *Collected Papers* (Martinus Nijhoff, The Hague, 1936), Vol. 2, p. 1.
[8] J. Pastrnak and K. Vedam, Phys. Rev. B **3**, 2567 (1971).
[9] J. H. Burnett, Z. H. Levine, and E. L. Shirley, US Patent No. 7,163,649 (B2) (16 January 2007).
[10] H. Sewell, US Patent No. 7,154,669 (B2) (26 December 2006).
[11] D. C. Allan, J. H. Bruning, and J. E. Webb, US Patent No. 6,785,051 (B2) (31 August 2004).
[12] D. C. Allan, N. F. Borrelli, C. M. Smith, and R. W. Sparrow, US Patent No. 6,649,326 (B2) (18 November 2003).
[13] D. C. Allan, N. F. Borrelli, C. M. Smith, and R. W. Sparrow, US Patent No. 6,806,039 (B2) (19 October 2004).
[14] C. W. Ponader, R. E. Youngman, and C. M. Smith, J. Am. Ceram. Soc. **88**, 2447 (2005).
[15] R. K. Chang, B. Lacina, and P. S. Pershan, Phys. Rev. Lett. **17**, 755 (1966).
[16] R. Dupree, A. P. Howes, and S. C. Kohn, Chem. Phys. Lett. **276**, 399 (1997).
[17] Z. Lin, M. E. Smith, F. E. Sowrey, and R. J. Newport, Phys. Rev. B **69**, 224107 (2004).
[18] A. Wong, A. P. Howes, R. Dupree, and M. E. Smith, Chem. Phys. Lett. **427**, 201 (2006).
[19] D. Laurencin, A. Wong, R. Dupree, and M. E. Smith, Magn. Reson. Chem. **46**, 347 (2008).
[20] D. Laurencin, A. Wong, J. V. Hanna, R. Dupree, and M. E. Smith, J. Am. Chem. Soc. **130**, 2412 (2008).
[21] J. M. Miller, Prog. Nucl. Magn. Reson. Spectrosc. **28**, 255 (1996).
[22] T. J. Kiczenski and J. F. Stebbins, J. Non-Cryst. Solids **306**, 160 (2002).
[23] E. Beck, Metallurgie (Halle) **5**, 514 (1908).
[24] E. Rumpf, Z. Phys. Chem. **B7**, 148 (1930).
[25] L. Vegard, Z. Phys. **5**, 17 (1921).
[26] E. G. Chernevskaya and G. V. Anan'eva, Sov. Phys. Solid State **8**, 169 (1966).
[27] R. W. Vaughan, D. D. Elleman, W.-K. Rhim, and L. M. Stacey, J. Chem. Phys. **57**, 5383 (1972).
[28] A. T. Kreinbrink, C. D. Sazavsky, J. W. Pyrz, D. G. A. Nelson, and R. S. Honkonen, J. Magn. Reson. **88**, 267 (1990).
[29] B. Bureau, G. Silly, J. Y. Buzaré, and J. Emery, Chem. Phys. **249**, 89 (1999).
[30] S.-H. Cai, Z. Chen, and H.-L. Wan, J. Phys. Chem. A **106**, 1060 (2002).
[31] H. S. Gutowsky and C. J. Hoffman, J. Chem. Phys. **19**, 1259 (1951).
[32] U. Groß, S. Rüdiger, A.-R. Grimmer, and E. Kemnitz, J. Fluorine Chem. **115**, 193 (2002).
[33] G. Engelhardt and D. Michel, *High-Resolution Solid-State NMR of Silicates and Zeolites* (Wiley, New York, 1987).
[34] K. J. D. MacKenzie and M. E. Smith, *Multinuclear Solid-State NMR of Inorganic Materials* (Pergamon, Oxford, 2002).
[35] J. Kudrnovský, N. E. Christensen, and J. Mašek, Phys. Rev. B **43**, 12597 (1991).
[36] J. N. Plendl, P. J. Gielisse, L. C. Mansur, S. S. Mitra, A. Smakula, and P. C. Tarte, Appl. Opt. **10**, 1129 (1971).